Here W_q occurs as defined by HS. The terms in the first curly bracket in the above expression can be combined with the other terms by integrating by parts with respect to k_y. Thus (h) reduces to the following form:

$$\frac{1}{2\pi^3}\int d\mathbf{k}\, f(W_q{}^0-\eta)\frac{e^2}{2m\hbar c^2}\frac{\partial}{\partial k_y}\langle q|Xp_xY+Yp_xX|q\rangle-\frac{e^2}{\hbar^2c^2}\frac{\partial W_q{}^0}{\partial k_y}\frac{\partial}{\partial k_y}\langle q|X^2|q\rangle$$

$$-\frac{e^2}{2mc^2}\langle q|Y^2|q\rangle-\frac{e^2}{2\hbar^2c^2}\frac{\partial^2 W_q{}^0}{\partial k_y{}^2}\langle q|X^2|q\rangle-\frac{e}{\hbar c}W_q{}^{(1)}\frac{\partial X_q}{\partial k_y}. \quad \text{(i)}$$

This is exactly the same expression as the contributions to χ from the remaining terms in (31), thus proving the equivalence of our result to that of HS.

PHYSICAL REVIEW VOLUME 136, NUMBER 3A 2 NOVEMBER 1964

Nuclear Magnetic Resonance Studies of the Metallic Transition in Doped Silicon*

R. K. SUNDFORS† AND D. F. HOLCOMB
Laboratory of Atomic and Solid State Physics, Cornell University, Ithaca, New York

(Received 12 June 1964)

The Si:P and Si:B systems have been studied using the methods of pulse and cw nuclear magnetic resonance. The purpose of this study is to investigate the transition of an impurity system in a solid from an array of isolated paramagnetic atoms or clusters of atoms to a superlattice of impurity atoms having strong wave-function overlap and metallic character. Knight shifts, line shapes, and nuclear spin relaxation times were measured for Si^{29} and B^{11} in p-type silicon and Si^{29} and P^{31} in n-type silicon. Phosphorus concentrations vary from 10^{17} to 10^{20} impurities/cm^3 and the temperature range investigated extends from 1.4 to 300°K. Onset of metallic behavior in n-type silicon at 4×10^{18} phosphorus impurities/cm^3 is indicated by the Si^{29} T_1 becoming proportional to T^{-1} between 1.4 and 4.2°K and by the existence of a Knight shift for Si^{29}. Above a phosphorus concentration of approximately 3×10^{19} cm^{-3}, Si^{29} T_1's and Knight shifts obey the Korringa relation. Broadening of the Si^{29} resonance line by 5 times the dipolar width and of the P^{31} resonance line by 100 times the dipolar width at concentrations of 1.4×10^{20} cm^{-3} is shown to be caused by fluctuations of the local Knight shift about the average Knight shift value. Such fluctuations are explained by a model of a Poisson distribution for the local P^{31} impurity density with a threshold local density of 3×10^{19} cm^{-3} for transition to metallic properties. This model agrees with the observed P^{31} resonance line shape and explains the transition to metallic behavior in n-type silicon. In p-type silicon, B^{11} and Si^{29} Knight shifts are measured for boron concentrations greater than 1×10^{19} cm^{-3}. The B^{11} T_1's and Knight shifts agree with the Korringa relation within a 15% experimental error. However, both the B^{11} T_1 and Knight shift are independent of concentration for boron concentrations between 2×10^{19} cm^{-3} and 8.5×10^{19} cm^{-3}. Such concentration independence may be explained by postulating a clustering of boron atoms at an average local density in a cluster greater than 8.5×10^{19} cm^{-3}. Wave function probability densities are calculated from Knight shifts with a free carrier density of states assumed valid. To facilitate comparison, wave-function densities are normalized per unit volume of the crystal and are 2600 cm^{-3} at P^{31} and 100 cm^{-3} at Si^{29} in n-type silicon and 80 cm^{-3} at Si^{29} in p-type silicon.

INTRODUCTION

THIS paper reports the experimental nuclear magnetic resonance (NMR) behavior of Si^{29}, P^{31}, and B^{11} nuclei in the silicon crystal lattice with increasing donor- or acceptor-impurity concentration. We are interested in those concentrations of impurities in which low-temperature electric resistivity and Hall-coefficient measurements indicate a transition from a nonmetal to a metal.[1] Graphs of the electrical resistivity as a function of temperature in n- and p-type silicon[2–6] and germanium[7,8] show three qualitatively different classes of behavior as the impurity concentration is varied. In n-type silicon at donor-impurity concentrations less than about 4×10^{18} cm^{-3}, the resistivity measurements[2,5] indicate that most of the electrons are bound to the impurity system at temperatures less than 20°K. We shall call this concentration range the *semiconducting*

* Work supported by the U. S. Office of Naval Research and the Advanced Research Projects Agency. The latter part of the work was also supported by the National Science Foundation.

† Present address: Washington University, St. Louis, Missouri.

[1] N. F. Mott and W. D. Twose, Advan. Phys. **10**, 107 (1961).

[2] G. L. Pearson and J. Bardeen, Phys. Rev. **75**, 865 (1949).
[3] F. J. Morin and J. P. Maita, Phys. Rev. **96**, 28 (1954).
[4] R. O. Carlson, Phys. Rev. **100**, 1075 (1955).
[5] R. K. Ray and H. Y. Fan, Phys. Rev. **121**, 768 (1961).
[6] G. A. Swartz, Phys. Chem. Solids **12**, 245 (1960).
[7] H. Fritzsche, Phys. Rev. **99**, 406 (1955).
[8] H. Fritzsche, Phys. Chem. Solids **6**, 69 (1958).

range in n-type silicon. At temperatures greater than 20°K in this semiconducting range, there is an exponential increase with temperature of the number of electrons in the conduction band. For concentrations between approximately 4×10^{18} cm^{-3} and approximately 10^{19} cm^{-3}, the resistivity is relatively small at the lowest temperatures and decreases slowly with increasing temperature. The model of an impurity band[9] growing in width with increasing concentration has been used in this *transition* range to explain the developing metallic character of the resistivity. Finally, for concentrations greater than approximately 10^{19} cm^{-3}, the resistivity is independent of temperature. In this *metallic* range, the impurity band is believed to have overlapped the conduction band and the crystal is a metal.

Bloembergen[10] first considered theoretically the Si^{29} NMR characteristics expected in n-type silicon in the three concentration ranges. At low temperatures in the semiconducting range, he anticipates being able to identify the paramagnetic nature of the donor atoms by means of the temperature and concentration dependence of the Si^{29} spin-lattice relaxation time T_1. The temperature and concentration dependence will be determined by the electron spin-lattice relaxation time for a given donor-impurity concentration. However, nuclear spin diffusion may limit this nuclear relaxation rate. In this case, the Si^{29} relaxation rate may be described by one of the cases discussed by Blumberg.[11] However, spin diffusion is dominant only when the fraction of the crystal volume in which the local magnetic fields of the impurities are larger than the dipolar fields is small compared to the total volume of the crystal. It can be shown that this condition is not satisfied for concentrations of phosphorus or boron in silicon greater than about 5×10^{17} cm^{-3}; hence, we do not expect to see effects of spin diffusion in our samples.

As the temperature is increased, in the semiconducting range, electrons are excited into the conduction band. These mobile electrons may then provide the most effective nuclear relaxation mechanism by means of the Fermi contact term of the hyperfine interaction. We may write this interaction as

$$\mathcal{H}=-(8\pi/3)\gamma_e\gamma_n\hbar^2\delta(\mathbf{r}_I)(\mathbf{I}\cdot\mathbf{S}), \qquad (1)$$

where γ_e and γ_n are the gyromagnetic ratios for the electron and nucleus, $\mathbf{S}$ and $\mathbf{I}$ are the electron and nuclear spin vectors, and $\delta(\mathbf{r}_I)$ is the Kronecker δ with origin of $\mathbf{r}_I$ at the nucleus. In the transition range at low temperatures and in the metallic range, the electron distribution is strongly degenerate. (Experimental values of the electrical conductivity allow one to infer a Fermi temperature of 38°K at 10^{18} electrons/cm^{-3} and of 176°K at 10^{19} cm^{-3}.) The most important pertinent features of NMR behavior expected for spin-$\frac{1}{2}$ nuclei are the following:

(1) When the nuclear magnetic moment interacts with a strongly degenerate distribution of mobile electrons, then the nuclear relaxation rate has a temperature dependence given by $1/T_1\propto T$.

(2) If the nuclear spins interact with the mobile electrons via the contact part of the hyperfine interaction and the electrons are described by a parabolic band, then the relaxation rate has a concentration dependence given by $1/T_1\propto N^{2/3}$, where N is the electron density. The contact term requires the presence of s character in the electron wave function as viewed from the nuclear site.

(3) If the mobile electrons are, in addition, independent, then the Knight shift K has the concentration dependence $K\propto N^{1/3}$. From the work of Pines,[12] it can be shown that if the motion of the electrons is correlated, then the Knight shift concentration dependence will differ from $N^{1/3}$.

(4) If the previous conditions apply, with the additional feature that the contact term is dominant in the relaxation rate, then the Korringa relation[13]

$$K^2=\frac{1}{T_1T}\frac{\hbar}{4\pi k}\left(\frac{\gamma_e}{\gamma_n}\right)^2 \qquad (2)$$

is obeyed. However, it should be noted that examination of the degree of departure from the Korringa relation is not a sensitive test of the degree of admixture of nonzero angular-momentum states in the wave function. This situation arises because of the relative ineffectiveness of relaxation by electrons in these higher angular momentum states.[14]

Schulman and Wyluda[15] performed the first experimental investigation of the Si^{29} resonance in n- and p-type silicon at 300°K for concentrations in the semiconducting range and extending into the transition range. They found the Si^{29} T_1 proportional to concentration as expected for a Boltzman distribution of mobile electrons.[10] At a given carrier concentration, the Si^{29} T_1 in p-type silicon was found to be eight times longer than in the n-type silicon. This difference was attributed to the presumably large p character in the hole wave function as seen from the Si^{29} nuclear site.

The NMR investigation reported in this paper includes measurements of T_1, T_2*, K and line shapes for P^{31} and Si^{29} resonances in Si:P and for B^{11} and Si^{29} resonances in Si:B. The time T_2* is a measure of the nuclear free-induction decay time following an rf pulse. Samples of Si:P with concentrations from 10^{17} to 10^{20} phosphorus impurities/cm^3 and of Si:B from 10^{18} to 10^{20} boron impurities/cm^3 were investigated. We

[9] T. Matsubara and Y. Toyozawa, Progr. Theoret. Phys. (Kyoto) **26**, 739 (1961).
[10] N. Bloembergen, Physica **20**, 1130 (1954).
[11] W. E. Blumberg, Phys. Rev. **119**, 79 (1960).
[12] D. Pines, in *Solid State Physics*, edited by F. Seitz and D. Turnbull (Academic Press Inc., New York, 1955), Vol. 1, p. 420.
[13] J. Korringa, Physica **16**, 601 (1950).
[14] A. H. Mitchell, J. Chem. Phys. **26**, 1714 (1957).
[15] R. G. Schulman and B. J. Wyluda, Phys. Rev. **103**, 1127 (1956).

measured Si^{29} T_1's at 1.6, 4.2, 20, 78, and 300°K. The B^{11} and P^{31} resonances were examined in the liquid-helium temperature range for concentrations greater than 10^{19} cm^{-3}.

We shall focus on three aspects of the silicon system. First, we shall show that a simple physical model for the local density distribution of donor impurities is indicated by the behavior of the P^{31} Knight shift and line shape and the Si^{29} Knight shift and linewidth. The model qualitatively explains the transition range in Si:P. Second, we discuss evidence for a clustering of boron atoms in the metallic range of Si:B. Finally, wave-function densities at the P^{31} and Si^{29} nuclei in Si:P and at the Si^{29} nucleus in Si:B are calculated from the measured values of the Knight shift.

The organization of the paper is as follows. In Sec. II we discuss the sample preparation, experimental equipment, and methods of measurement. In Sec. III we initially study the NMR behavior of Si:P. Resonance line broadening is shown to be caused by a distribution of Knight shifts. The model for the distribution of P^{31} impurities is developed. In Sec. IV the NMR behavior of Si:B and distribution of impurities are discussed. In Sec. V we calculate the wave function probability densities. In Sec. VI we summarize the paper.

II. EXPERIMENTAL PROCEDURES

A. Samples

Samples of Si:P and Si:B were chosen which have phosphorus or boron concentrations spaced along the transition from nonmetallic to metallic properties. Donor or acceptor concentrations were determined from room-temperature resistivity measurements made by the supplier and then by extrapolation from the resistivity versus concentration curves of Irvin.[16] Arc spectra determinations of the impurity-atom density were also made for the samples of the highest concentrations. Resistivities of the Si:P crystals at room temperature were measured by the four-point probe method[17] prior to sample preparation.

Sample preparation included crushing about 2 g of a silicon crystal to a particle size much less than the skin depth. (The skin depth at 10 Mc/sec with 10^{20} electrons/cm^3 is about 0.4 mm.) The resulting silicon powder was mixed with melted paraffin wax in a cylindrical mold to form a sample.

Arc spectra measurements showed impurities other than boron in amounts varying from sample to sample in p-type silicon. In addition, electron spin resonance (ESR) spectra of several p-type samples revealed the presence of two paramagnetic impurity resonances with g values of approximately two.

Samples[18] of cubic BN and GaP were used as reference standards for the B^{11} and P^{31} Knight shifts, respectively. Silicon samples with their identification symbols, source symbols, room-temperature resistivities, and concentrations are listed in Table I.

TABLE I. Si:B and Si:P samples. The error in concentration is ±10%.

Identification symbol[a]	Supplier symbol[b]	Resistivity (Ω-cm)	Donor or acceptor concentration (10^{17} cm^{-3})
P-1	*ay*	0.00068	1400
P-2	*ay*	0.00087	900
P-3	*sm*	0.00178	450
P-4	*ay*	0.0045	180
P-5	*ay*	0.0064	110
P-6	*ay*	0.0090	60
P-7	*ay*	0.0151	25
P-8	*ay*	0.025	11
P-9	*ay*	0.046	3.2
P-10	*ay*	0.080	1.2
B-1	*cl*	0.0014	850
B-2	*cl*		270[c]
B-3	*cl*	0.0053	210
B-5	*cl*	0.018	54
B-7	*cl*	0.033	24
B-9	*cl*		0.01[d]

[a] Samples designated P are n-type silicon with phosphorus impurities. Those samples designated B are p-type samples with boron impurities.
[b] Samples *ay* were obtained from Allegheny Electronic Chemicals Company; sample *sm* was contributed by Semi-Metals, Incorporated; samples *cl* were contributed by Dr. R. O. Carlson of General Electric Research Laboratories.
[c] Sample concentration determined from arc spectra measurements.
[d] Concentration estimated from boron impurity added in sample preparation.

B. Experimental Equipment and Method of Measurement

An NMR pulse apparatus[19] with gated amplifier and phase coherent detection[20] was used with a gated integrator[21] for T_1, T_2*, and K measurements. The external magnetic-field stability was maintained within short term field fluctuations of five parts in 10^6 by use of an accessory gaussmeter and frequency counter. A sample changer similar to those used by Bloembergen[22] and Fuschillo[23] was constructed. The sample changer, with the addition of a heater and temperature sensors, formed a probe[24] placed in a standard double Dewar system.

The T_1 measurements were usually made in the following way. A series of more than ten 90° pulses with time spacing much greater than T_2* but much less than T_1 saturated the nuclear spin system. At a time τ later, another 90° pulse was applied and the amplitude of the free-induction decay following this pulse was measured as a function of τ by sampling a portion of the decay with the gated integrator.

[16] J. C. Irvin, Bell System Tech. J. **41**, 387 (1962).
[17] L. B. Valdes, Proc. IRE **42**, 420 (1954).
[18] Samples of (cubic) BN and GaP were loaned to us by General Electric Research Laboratories.
[19] W. G. Clark, thesis, Cornell University, 1961 (unpublished).
[20] J. J. Spokas and C. P. Slichter, Phys. Rev. **113**, 1462 (1959).
[21] R. J. Blume, Rev. Sci. Instr. **32**, 1016 (1961).
[22] N. Bloembergen, Physica **15**, 386 (1949).
[23] N. Fuschillo, Rev. Sci. Instr. **27**, 394 (1956).
[24] R. K. Sundfors, thesis, Cornell University, 1963 (unpublished).

We measured T_2^* from photographs of the free induction decay following an rf pulse. The shape of the free-induction decay is the Fourier transform of the absorption line shape function.[25]

Knight shifts were measured by observing the resonance magnetic fields of both the reference resonance and the shifted resonance at constant frequency of the pulse apparatus. The resonance-field value itself was measured with the accessory gaussmeter and frequency counter and could be determined within 5% of the linewidth or 0.05 G, whichever was larger. Knight shifts of as many as five different samples could be compared with a reference sample at a given temperature by using the sample changer.

The P^{31} resonance was studied with cw techniques at 4.2°K with a Varian spectrometer, Model 4210A. A finger Dewar designed by Schreiber was placed in the spectrometer crossed-coil probe to achieve low temperatures. The presence of B^{11} and Si^{29} in the Pyrex of the Dewar prevented its use for these nuclei.

III. THE DISTRIBUTION OF IMPURITIES IN *N*-TYPE SILICON

A. Experimental NMR Characteristics

We shall first discuss the nature of the experimental NMR data in the Si:P system. The main import of this discussion is to identify the concentration range in which a well-developed metallic behavior exists. Detailed analysis will be applied only to line broadening and Knight shift data in this metallic range. This analysis will then be used as the basis for development of a model for the spatial distribution of phosphorus impurities. Aspects of the data bearing on properties of the electron wave functions will be analyzed in Sec. V.

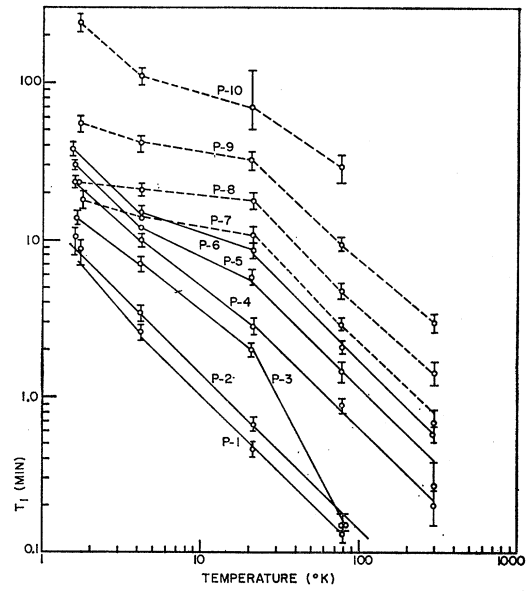

FIG. 1. Temperature dependence of Si^{29} T_1's for Si:P samples.

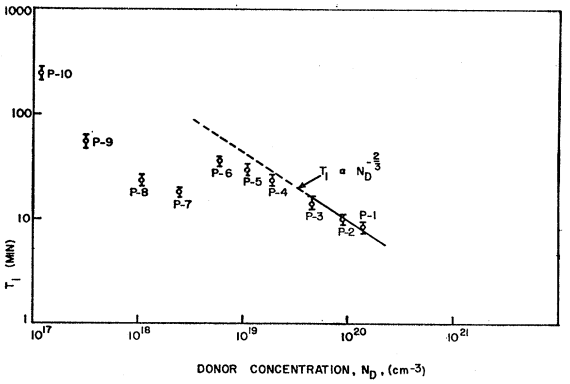

FIG. 2. Concentration dependence of Si^{29} T_1's in Si:P at 1.6°K.

The Si^{29} relaxation time, Knight shift, and linewidth data all exhibit effects identifiable with the three concentration ranges, *metallic*, *transition*, and *semiconducting*. In Fig. 1, the Si^{29} T_1 is plotted as a function of temperature for a range of concentrations. For ease in identification, T_1 values of samples in the semiconducting range are connected by dotted lines. Values of T_1 for samples in the other two ranges are connected by full lines. For sample P-3, the temperature dependence is somewhat anomalous compared to the other samples, especially above 20°K. This behavior is believed to be associated with paramagnetic impurity content in addition to the P^{31} nuclei in sample P-3.

It should be noted that for all spin systems examined in this work, the relaxation times are sufficiently long that the assumption of a single T_1, that is, that a common spin temperature obtains for the whole system, seems reasonable. It is true, of course, that individual nuclear spins see various interaction strengths. No departure from exponential recovery of the magnetization was observed.

In Fig. 2, the Si^{29} T_1 at 1.6°K is plotted as a function of donor concentration. The nature of the temperature dependence for various samples in Fig. 1 and the nature of the concentration dependence in Fig. 2 both exhibit characteristic changes at donor concentrations of about 4×10^{18} cm^{-3} and 3×10^{19} cm^{-3}. For concentrations above 3×10^{19} cm^{-3}, Fig. 1 shows that T_1 is proportional to T^{-1} and Fig. 2 shows T_1 proportional to $N_D^{-2/3}$, where N_D is the donor concentration. This is the concentration range in which the resistivity data indicate metallic behavior. The relaxation time behavior is, as noted in the Introduction, that expected for a situation in which the nuclei are relaxed by the Fermi contact interaction with a highly degenerate distribution of electrons with a density of states appropriate to electrons in a parabolic band. The T^{-1} dependence of T_1 carries into the transition range, as we see in Fig. 1. But the concentration dependence exhibited in Fig. 2

[25] I. J. Lowe and R. E. Norberg, Phys. Rev. **107**, 46 (1957).

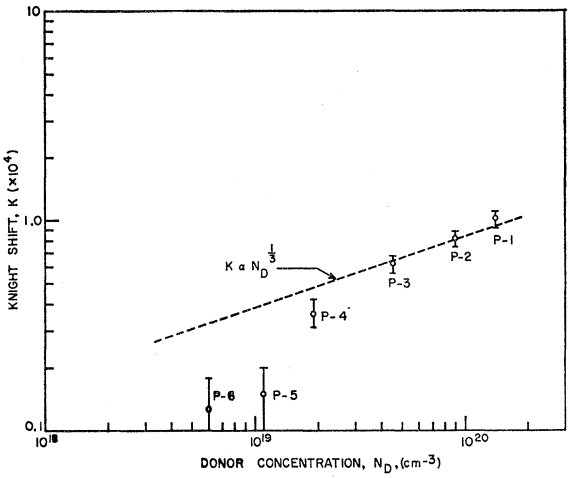

FIG. 3. Concentration dependence of Si^{29} Knight shifts in Si:P at 1.6°K.

departs from the characteristic metallic behavior below about 3×10^{19} cm^{-3}.

In Fig. 3, the Si^{29} resonance-line field shift at 1.6°K is plotted as a function of the donor concentration. The metallic nature of the system in this concentration range, indicated by the resistivity and T_1 data, suggests the identification of this shift with the Knight shift. The Knight shift is first observable at the beginning of the transition range and becomes proportional to $N_D^{1/3}$ in the metallic range. The data in the transition range fall below the extrapolation of the $N_D^{1/3}$ line from the metallic range, indicating that not all of the donor atoms contribute electrons to the free electron system.

Use of the Korringa relationship, Eq. (2), together with the experimental data for T_1, allows the calculation of a theoretical value of the Knight shift. Table II shows the calculated and measured values of K and their ratio for samples in the transition and metallic ranges. We note the increasingly good agreement between calculated and measured values of K. The good agreement in the metallic range provides further evidence that conditions (1) through (4) listed in Sec. I are all satisfied.

TABLE II. Comparison of the measured Si^{29} linewidths and Knight shifts in Si:P. Comparison of computed and measured Knight shift values.

Sample	Measured Si^{29} T_1 at 4.2°K (min)	Calculated K (10^{-4})	Measured K (10^{-4})	Ratio measured K to calculated K	Linewidth at 10 kG (G)
P-1	2.6	1.01	1.03	1.0	0.98±0.10
P-2	3.4	0.88	0.81	0.92	0.84±0.08
P-3	7.0	0.62	0.60	0.98	0.73±0.07
P-4	10.0	0.52	0.21	0.40	0.65±0.06
P-5	12.0	0.47	0.12	0.26	0.50±0.05
P-6	15.0	0.42	0.07	0.17	0.38±0.08
P-7	14.0		0.0	0.0	0.38±0.08
P-8	21.0		0.0	0.0	0.20±0.02
P-9	41.0		0.0	0.0	0.20±0.02
P-10	101.0		0.0	0.0	0.20±0.20

Table II also lists Si^{29} linewidths for various samples. These linewidths were obtained from the experimental free induction decay times T_2^*. The decays were approximately exponential, indicating a Lorentzian line shape.[25] Thus, the absorption linewidth between half-maximum points is given by the relation $\delta H=2(\gamma_n T_2^*)^{-1}$. We note that in the semiconducting range, the line width is constant and equal to 0.20 G. This value is appropriate for nuclear magnetic dipolar broadening within the Si^{29} system. The broadening of the resonance line at higher concentrations is correlated with the growth of K and suggests a distribution of Knight shifts for the Si^{29} system in the transition and metallic ranges.

The P^{31} resonance was observed with both pulse and cw techniques in samples P-1 and P-2 at liquid-helium temperatures. Although the signal-to-noise ratio available predicted observability of the resonances in samples P-3 and P-4 with the cw apparatus, they could not be seen. The measured P^{31} T_1 for both samples is 0.4±0.15 sec at 1.6°K and the product T_1T is constant in the 1.4° to 4.2°K temperature range. Values of K obtained in cw experiments were 25×10^{-4} for sample P-2 and 27×10^{-4} for sample P-1, with estimated uncertainties of 10%. The short T_1's and large values of K show a much larger Fermi contact interaction at the P^{31} nuclei than at the Si^{29} nuclei. Within the rather large experimental errors, the Korringa relation between T_1 and K is obeyed and the values of K are proportional to $N_D^{1/3}$.

The P^{31} resonance line for sample P-1 is shown in Fig. 4. The trace was obtained in the dispersion mode under conditions of slow passage, fast modulation, a saturating rf field H_1, and phase-sensitive detection at 4.2°K. The resonance field H_0 is 4.7 kG. The Knight shift is measured from the reference P^{31} resonance in GaP to the peak of the P^{31} resonance in Si:P. The expected dipolar linewidth for the P^{31} system is about 0.1 G. The measured width between half-maximum points in Fig. 4 is 11 G, about 100 times the dipolar width.

B. Line Broadening and the Knight Shifts

Several aspects of the experimental data confirm the presumption that the Si^{29} and P^{31} line broadening in the

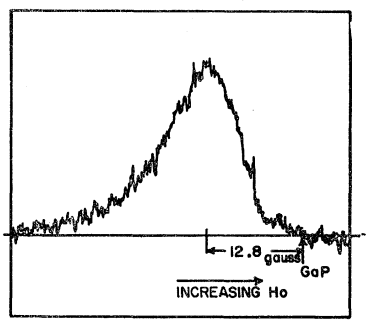

FIG. 4. Recorder NMR dispersion mode P^{31} derivative for sample P-1 at H_0=4.65 kG and at 4.2°K.

transition and metallic ranges arises from a distribution of values of K.

The P^{31} linewidth in sample P-1 was measured at two values of H_0, 4.65 and 3.14 kG. The linewidth was found to be proportional to H_0, as should be the case for a linewidth determined by a distribution of values of K.

For both P^{31} and Si^{29}, the ratio of linewidth to magnitude of field shift is found to be the same. For P^{31} at 4.65 kG the ratio is 11.0 G/12.8 G=0.86. For Si^{29} in sample P-1, one must make a small correction for contribution from the dipolar width. Since the line shape is Lorentzian, we subtract the low-concentration linewidth, 0.20 G, from the observed value of 1.0 G at 10 kG. The ratio of linewidth to field shift for Si^{29} is then 0.8 G/0.97 G=0.82. These similar ratios for P^{31} and Si^{29} for greatly different magnitudes of linewidth are consistent with assignment of a distribution of values of K as the source of the broadening.

Finally, we have experimental evidence that the P^{31} resonance line is inhomogeneously broadened. The P^{31} dispersion mode signal shown in Fig. 4 was observed with a saturating rf field H_1. No absorption mode signal could be observed, but the amplitude of the dispersion mode signal was proportional to H_1. These characteristics are appropriate to the inhomogeneously broadened line.[26] Let us suppose that because of the inhomogeneity of the donor-impurity distribution, there are fluctuations of the Knight shift about some average value determined by the average concentration. Parts of the crystal which have the same resonance-line position contribute a *spin packet* of dipolar width 0.1 G to the resonance. Under conditions of fast modulation and saturation, the dispersion derivative signal of such a spin packet will look something like the sketch in Fig. 5, based on the theory of Redfield.[27] (Such dispersion derivatives can easily be observed experimentally in appropriate nuclear spin systems.) We see that the sum of such spin packet contributions can form the rather peculiar dispersion line shape derivative shown in Fig. 4.

C. A Model for Distribution of Impurities

1. The Knight Shift Distribution

The conclusion that the P^{31} line shape arises from a distribution of Knight shifts suggests the possibility of using this distribution to infer the probability distribution of local impurity densities. For this purpose, we need a scheme for associating a certain position on the Knight shift distribution with a particular local concentration. Then the relative amplitude of the resonance at that point is a measure of the probability of a P^{31} nucleus lying in a region of that local concentration.

The expression for the Knight shift can be written in the form

$$K=(8\pi/3)\chi_p P_F', \tag{3}$$

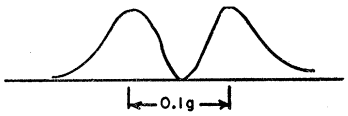

FIG. 5. Expected NMR dispersion mode derivative of "spin packet" contribution to the line shape of Fig. 4.

where P_F' is the mean wave-function probability density at the Fermi surface normalized in unit volume of the crystal, and χ_p is the electron spin susceptibility per unit volume.

For our present purposes it is most illuminating to write χ_p in the form

$$\chi_p=N(g\beta\langle S_z\rangle_{\rm av}/H_0), \tag{4}$$

where N is the number of electrons per unit volume and $\langle S_z\rangle_{\rm av}$ is the expectation value of the electron spin quantum number S_z averaged over all electrons. We note that the electron-spin flip time $(T_1)_e$ is almost surely much longer than the time for an electron to move from one P^{31} impurity atom to the next.[28] This transit time is about 5×10^{-14} sec at 10^{19} electrons per cm^3. Hence, the polarization factor $\langle S_z\rangle_{\rm av}$ is determined over long distances in the crystal, and represents to all intents and purposes an average value for the whole crystal. N, on the other hand, is the *local* electron density. (The question of the appropriate volume over which to measure N is considered in the next subsection.) Our conclusion is that the local fluctuations in χ_p will simply be determined by local fluctuations in N.

Provided the P^{31} nuclei are not packed together too tightly, P_F' will not depend strongly on the local density, because of the dominant influence of the small central core. We make the simplifying assumption that P_F' is, in fact, constant.

Using the presumption that local electron concentrations are equal to local P^{31} "ion" concentrations, plus the considerations of the above two paragraphs, Eq. (3) now gives us the direct proportionality, $N_{P^{31}}=CK$. We determine the constant C by identifying the mean of the Knight shift distribution with the average density, 1.4×10^{20} cm^{-3} for P-1 and 9×10^{19} cm^{-3} for P-2.

We should note that the argument in the preceding paragraphs does not contradict the conclusion that the *mean* value of K is proportional to $\langle N\rangle_{\rm av}^{1/3}$. Although, as noted, the value of K at any P^{31} nucleus is proportional to the local concentration N when we change $\langle N\rangle_{\rm av}$ we also change $\langle S_z\rangle_{\rm av}$. In the free-electron gas, for example, we have

$$\langle S_z\rangle_{\rm av}=\tfrac{3}{2}(\mu^2H/g\beta E_F)$$

[26] A. M. Portis, Phys. Rev. **91**, 1071 (1953).
[27] A. G. Redfield, Phys. Rev. **98**, 1787 (1955).

[28] R. C. Fletcher, W. A. Yager, G. L. Pearson, and F. R. Merritt, Phys. Rev. **95**, 844 (1954). These authors report observation of the conduction electron resonance line at 6×10^{18} P/cm^3, with a linewidth less than 3 Oe, at 4.2°K. This implies that $(T_1)_e\gtrsim3\times10^{-8}$ sec at this concentration. We are not aware of measurements at higher concentration, but shortening of $(T_1)_e$ below 10^{-11} sec in our concentration range seems unlikely.

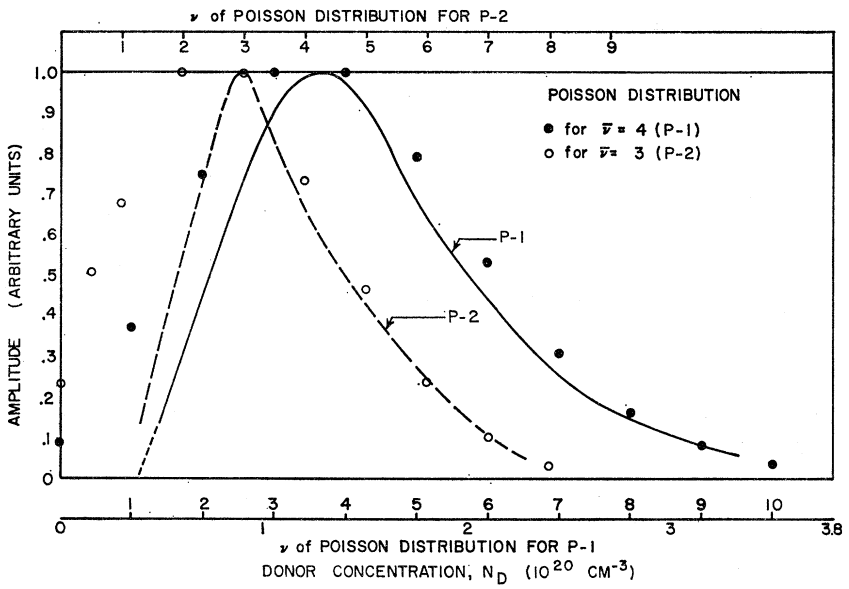

FIG. 6. Comparison of P^{31} line shape with Poisson distribution. Solid line is P^{31} line shape of Fig. 4 compared with Poisson distribution with $\bar{\nu}=4$. Dashed line is P^{31} line shape for P-2 compared with Poisson distribution with $\bar{\nu}=3$.

and E_F is proportional to $N^{2/3}$. Thus, we still expect the mean value of χ_p to change as $\langle N\rangle_{\text{av}}{}^{1/3}$.

On the basis of Eq. (3), we can transcribe the experimental P^{31} line shape from Fig. 4 and a similar experimental trace for sample P-2 directly into an experimental local density distribution. These are shown as the solid and dashed lines, respectively, in Fig. 6.

2. *The Poisson Model*

We now develop a model for the distribution of impurities based on simple physical assumptions. First, we assume that both the P^{31} and Si^{29} atoms are randomly distributed. Such an assumption is surely accurate for the 4.6% abundant Si^{29} atoms, and, depending on the manner of doping, may be a good approximation for the P^{31} atoms.

For our second assumption, we use the hypothesis of Mott[29] that there must be a minimum electron density below which the metallic state will not form. Mott shows that this condition for the minimum electron density N_m can be written, in general, as

$$N_m{}^{1/3}a_H \gtrsim 0.25\,, \tag{5}$$

where

$$a_H=\hbar^2 k_D/m_d{}^*e^2. \tag{6}$$

$m_d{}^*$ is some appropriate effective mass, and k_D is the dielectric constant. However, it is found experimentally that, in n- and p-type silicon and germanium, N_m will fall correctly at a concentration in the transition range if the criterion is written $N_m{}^{1/3}a_H \gtrsim 0.2$. In this expression, a_H is the Bohr radius appropriate to the particular donor or acceptor ionization energy. For our model, $m_d{}^*$ is the appropriate density-of-states effective mass, taking into account the band minima. This value is $m_d{}^*=1.08m_0$ for electrons in silicon. Identification of the transition point with the experimentally observed lower end of the metallic range, at 3×10^{19} cm^{-3}, gives for our case the condition

$$N_m{}^{1/3}a_H \gtrsim 0.17\,. \tag{7}$$

This metallic threshold density is in agreement with the straightforward interpretation of the resistivity results[2,5] in n-type silicon and the Si^{29} NMR results reported in this paper.

The threshold density obtained above corresponds to a uniform distribution of closely packed spheres of radius 20 Å. This sphere we now take to be the *critical volume* for consideration in our model. We reason that significant electron wave-function overlap of two nearby impurity *atoms* is the appropriate criterion for contribution to the local N, just as it is for the Mott condition. We establish ourselves at one P^{31} nucleus and take such a sphere surrounding the base nucleus. Then we assume that the base nucleus plus other P^{31} nuclei within that volume will contribute electrons to the electron density at the base nucleus and any outside of the critical volume will not do so. Thus, our problem reduces to one of finding the probability distribution for having a given number of nuclei in that critical volume. For a large number of atoms randomly placed in the lattice, the fluctuations about the average number of atoms in a given volume is described by the Poisson distribution, if the average number of atoms in the given volume $\bar{\nu}$ is small. In the two samples of interest, P-1 and P-2, the average numbers of atoms in the critical volume are about 4 and 3, respectively.

In Fig. 6 we plot the Poisson distribution of the number of P^{31} atoms in a critical volume, identifying

[29] N. F. Mott, Phil. Mag. **6**, 287 (1961).

the mean value $\bar{\nu}$ with the average density for sample P-1, 1.4×10^{20} cm^{-3}. We have normalized the curve so that its peak height corresponds with the peak of the experimental density distribution curve derived from the Knight-shift distribution for this sample. The same thing has also been done for sample P-2 at 9×10^{19} cm^{-3}, and the vertical scale of this curve is also normalized against the peak of the experimentally obtained curve for this sample.

In comparing both pairs of curves in Fig. 6, we note that there is good agreement between the curves for $\nu\gtrsim\bar{\nu}$. However, there is a cutting off of the experimental curve compared with the Poisson curve for $\nu<\bar{\nu}$ at a concentration of about 2 to 4×10^{19} cm^{-3}. This cutoff is expected from Mott's hypothesis. Nuclei of P^{31} in regions of local density less than 3×10^{19} cm^{-3} should not contribute to the P^{31} metallic resonance. It is interesting to note that this explanation is consistent with our inability to observe the P^{31} resonance in samples P-3 and P-4.

The agreement in Fig. 6 between the experimentally derived curve and that based on the idea of the critical volume and the Poisson distribution is encouraging. However, one should observe that the fit is not extremely sensitive to the value of $\bar{\nu}$. The mean value $\bar{\nu}$ could vary by one unit without significantly worsening the fit. The size we have chosen for the critical volume is clearly only plausibly justified. But one cannot escape the feeling that the excellent reproduction of the asymmetry and the large linewidth of the P^{31} resonance gives considerable credence to the gross features of the Poisson model.

An approach very similar to our preceding model has been used by Kane[30] to calculate the total density of states in a highly impure semiconductor. In order to describe the band character, Kane considers fluctuations in local impurity potential energy due to fluctuations of the local impurity-atom density. His characteristic volume, a sphere of radius equal to the Fermi-Thomas screening length, is of the same order of magnitude as our critical volume.

The Poisson model which we have used to explain the P^{31} line shape and linewidth can also be applied to explain in a qualitative way the transition range in Si:P. The transition range begins at about 4×10^{18} cm^{-3} with the first signs of metallic behavior in the NMR properties. For an average concentration of 4×10^{18} cm^{-3}, the appropriate Poisson distribution of impurities is one with $\bar{\nu}=0.1$. For such a Poisson distribution about 1% of the crystal has local densities larger than 3×10^{19} cm^{-3}. As the average concentration of impurities is increased through the transition range, the fraction of the crystal volume having local densities greater than 3×10^{19} cm^{-3} increases rapidly. At the average concentration of 3×10^{19} cm^{-3} over 60% of the volume of the crystal has such densities.

[30] E. O. Kane, Phys. Rev. **131**, 79 (1963).

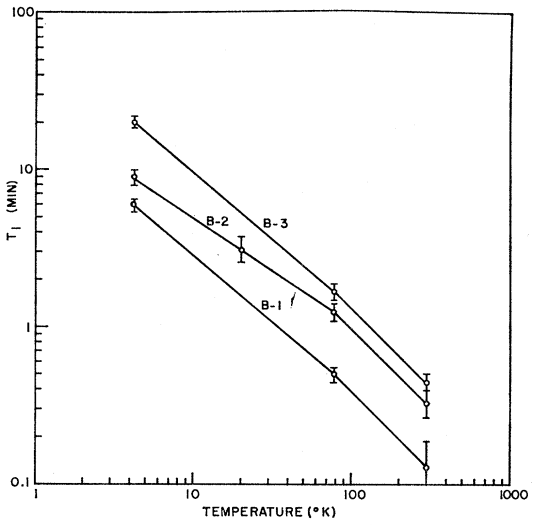

FIG. 7. Temperature dependence of Si^{29} T_1's in Si:B for boron concentrations greater than 1×10^{19} cm^{-3}.

IV. *P*-TYPE SILICON

A. Experimental Electrical and NMR Characteristics

As noted in Sec. I the experimental electrical resistivity dependence on temperature in Si:B[4] also shows three classes of behavior as the boron concentration is varied. The transition range extends from about 3×10^{18} cm^{-3} to about 1×10^{19} cm^{-3}.

An NMR study of the Si^{29} resonance in Si:B similar to that in Si:P was hampered by the presence of paramagnetic impurities in addition to boron acceptors. The magnitude of this paramagnetic impurity content was observed from ESR measurements to vary from sample to sample and was estimated to be larger than 10^{17} cm^{-3} in some samples. The measured Si^{29} T_1 dependence on temperature is irregular and varies from sample to sample in the semiconducting and transition ranges. An explanation of this behavior is that the nuclear relaxation rate due to the paramagnetic impurity is of the same magnitude as the relaxation rate due to the boron content alone. We shall not consider the T_1 data in the transition and semiconducting ranges further.

In Fig. 7 we plot the Si^{29} T_1 as a function of temperature for three samples in the metallic range. All three samples give $T_1\propto T^{-1}$ above 78°K, but have slower temperature dependences below 78°K. We interpret this behavior to mean that only above 78°K does the Fermi contact interaction dominate the nuclear relaxation. Above 78°K, the concentration dependence is consistent with the relation $T_1\propto N_A^{-5/6}$ where N_A is the acceptor concentration. If condition (2) of Sec. I also applied to holes in the metallic range, we would expect $T_1\propto N_A^{-2/3}$.

The Si^{29} Knight shifts for samples B-1 and B-3

TABLE III. Comparison of the measured Si^{29} linewidths and Knight shifts in Si:B. Comparison of computed and measured Knight shift values.

Sample	Measured Si^{29} T_1 at 78°K (min)	Calculated K (10^{-4})	Measured K (10^{-4})	Linewidth at 10 kG (G)
B-1	0.50±0.05	0.40±0.02	0.33±0.05	0.50±0.05
B-3	1.70±0.20	0.22±0.01	0.21±0.05	0.38±0.04
B-5				0.31±0.04
B-7				0.23±0.02
B-9			0.0	0.20±0.02

measured at 4.2°K are shown in the fourth column of Table III. The concentration dependence is consistent with the relation $K \propto N_A^{1/3}$. In the second column of Table III the measured Si^{29} T_1's at 78°K are listed. Column three lists values of K computed from these measured T_1's by use of the Korringa relation.

The Si^{29} NMR behavior in Si:B agrees with conditions one and three of Sec. I. The $N^{-5/6}$ concentration dependence of the Si^{29} T_1 is an indication of appreciable p character in the hole wave function. Mitchell[14] shows that the noncontact part of the hyperfine interaction is characteristically much less effective than the contact part. He shows also that the noncontact and contact terms give the same temperature dependence for the nuclear T_1, $T_1 \propto T^{-1}$. However, the noncontact term gives a much faster concentration dependence N^2 to the noncontact part of the relaxation rate. In Table III, the disagreement between the calculated and measured values of K for sample B-1 could be explained by the effect of the noncontact term in the nuclear relaxation rate.

The fifth column of Table III lists the Si^{29} linewidths calculated from the experimental free-induction decay time T_2^* as was done for Si:P. The decays are exponential, indicating a Lorentzian line shape. Again, a distribution of Knight shifts in the transition and metallic ranges is suggested by the correlation between the resonance line broadening and the Knight shift.

The B^{11} resonance was observed only with pulse methods for samples in the metallic range at liquid-helium temperatures. Between 1.4 and 6°K, experimental B^{11} T_1's are proportional to T^{-1}. At 4.2°K, the measured B^{11} T_1 is concentration-independent for samples B-1, B-2, and B-3 and is equal to 2.0±0.2 min. Experimental values of B^{11} Knight shift are also concentration-independent and shown in Table IV. Solid $NaBH_4$ and BN (cubic) have nearly perfect cubic symmetry at the boron site and are used as reference samples. The B^{11} T_1 and K do obey the Korringa relation within the experimental uncertainty of about 15%.

TABLE IV. Measured values of the B^{11} Knight shift at 4.2°K in Si:B.

Sample	Knight shift (10^{-4})
$NaBH_4$	0
BN (cubic)	0
B-3	0.65±0.05
B-1	0.65±0.05

Both B-1 and B-3 have B^{11} linewidths of 0.30±0.05 G, and the free-induction decay shapes are approximately exponential. These linewidths appear to be broadened since the anticipated dipolar broadened line is about 0.1 G. It was not possible to study the B^{11} resonance line under conditions of slow passage because of the long B^{11} T_1 at 4.2°K.

B. The Boron Impurity Distribution

Line broadening in Si:P arises from a distribution of Knight shifts. In Si:B, we have seen that there is a Si^{29} line broadening in the transition and metallic ranges similar to that in Si:P. The ratio of Si^{29} line broadening to Knight shift in gauss is also similar to the ratios found in Sec. IIIB. For sample B-1, the Si^{29} line width is 0.50 G at 10 kG. Since the line shape is Lorentzian, we subtract the low-concentration line width of 0.20 G. The ratio of line broadening to Knight shift is then 0.30 G/0.33 G=0.90. From the similarity of this ratio and of the line broadening in Si:P and Si:B, it seems reasonable to attribute line broadening in Si:B also to a distribution of Knight shifts.

However, the distribution of boron impurities, at least in the metallic range of Si:B, does not appear to be random. The concentration independence of the B^{11} T_1 and K is in conflict with an assumption of randomness and indicates that the average local hole density at the B^{11} site is independent of concentration over the range measured, from 2.1×10^{19} to 8.5×10^{19} boron atoms/cm^3. On the other hand, the Si^{29} T_1, K, and line broadening are concentration-dependent. This Si^{29} NMR behavior indicates that the average local hole density at the Si^{29} site is roughly proportional to the average boron concentration.

The B^{11} and Si^{29} NMR behavior can be understood if boron acceptors form *dense clusters* in the metallic range with an average local density in a cluster greater than 8.5×10^{19} cm^{-3}. (This last concentration is the largest boron concentration measured in our samples.) Addition of boron impurities results in the increase in volume but not of average local hole density in such dense clusters. Therefore, the B^{11} nuclei sample an average local hole density which is independent of concentration. However, the randomly distributed Si^{29} nuclei will have positions both inside and outside of these dense clusters of boron. The average local hole density seen by the full Si^{29} nuclear system will therefore be determined by the average boron concentration.

To support this interpretation, there is evidence of lattice changes in samples of silicon with diffused boron layers from the experimental x-ray diffraction measure-

ments of Miller, Moore, and Moore.[31] They prepared thin slices of silicon crystal with a thin diffused layer of boron at surface concentrations of boron lying within what we call the transition and metallic ranges. From 8×10^{18} cm^{-3} to 3×10^{19} cm^{-3}, they measured a rapid increase in diffracted x-ray intensity and at 8×10^{18} cm^{-3} they computed the lattice stress to be 3×10^{9} dynes/cm^2. They associate these characteristics with the generation of slip dislocations throughout the volume of the crystal.

If similar changes in structure occur in bulk Si:B, presumably arising from the small boron atomic volume, then they may provide a mechanism by which boron impurities would cluster. The B^{11} NMR data supports the presumption that the boron impurities in such dense clusters still occupy substitutional sites of cubic symmetry in the silicon lattice. If boron atoms did not occupy sites of cubic symmetry, the resultant electric field gradients should clearly show up in quadrupole broadening of the resonance line.

V. THE WAVE FUNCTION IN THE METALLIC STATE

Knight-shift measurements provide information about the wave function density at the Si^{29} and P^{31} sites in Si:P and at the Si^{29} site in Si:B through Eq. (3). We use the wave function probability density normalized in unit volume of the crystal P_F' to facilitate comparison. The theoretical paramagnetic spin susceptibility per unit volume, χ_P, is given in Eq. (4). It may be written in the form

$$\chi_P=3\left(\frac{GF}{6\pi^2}\right)^{2/3}m^*\frac{\mu^2}{\hbar^2}\langle N\rangle_{\rm av}^{1/3}, \tag{8}$$

where μ is the appropriate electron or hole magnetic moment, m^* is the density-of-states effective mass, F is the number of band minima or maxima, and G is the total orbital and spin degeneracy. For electrons in silicon, we use the following values: $F=6$, $G=2$, and $m^*=0.33m_0$.

To obtain the magnetic moment of the hole, we use a g value of 1.9. Feher, Hensel, and Gere[32] observed an anisotropic hole g value under an applied external stress approximately equal to that which Miller, Moore, and Moore[31] indicate exists in the metallic range in boron-doped silicon. The value $g=1.9$ is the average over angle of the anisotropic g value of Feher, Hensel, and Gere. Under the condition of large stress, we expect the following values for holes: $F=1$, $G=2$, and $m^*=0.55m_0$.

In calculating the wave-function probability densities using Eqs. (3) and (8), we assume the mobile carriers are independent, and that each acceptor or donor contributes one carrier. The wave-function density is calculated for the mean Knight shift corresponding to the average density of P^{31} impurities in sample P-1 and the average density of boron impurities in sample B-1. In Table V, we list these calculated wave-function densities normalized in unit volume. Normalized in this way, the numbers in the table also give the factor by which the wave-function probability density is enhanced over the value appropriate to a uniform spread throughout the crystal. We have not calculated the wave-function density from the B^{11} Knight shift since we do not know the appropriate average local hole density at the B^{11} site, because of the unknown nature of the clusters.

TABLE V. Values of wave-function probability density normalized in unit volume, calculated from the measured Knight shifts in samples P-1 and B-1.

Sample	Nucleus	P_F'
P-1	P^{31}	2600±300
	Si^{29}	100±10
B-1	Si^{29}	80±10

The value of 100 cm^{-3} for the wave-function probability density at Si^{29} in Si:P may be compared with the value found from the data of Schulman and Wyluda[15] in nondegenerate samples with thermally excited electrons. The data of Schulman and Wyluda or our room-temperature T_1 data for samples P-9 and P-8 used with the theoretical expression for T_1 in semiconductors given by Abragam[33] give a wave-function probability density at the Si^{29} site of approximately 130 cm^{-3}. This value is in fair agreement with our Knight shift determined value for P_F'.

It is to be noted that the value of P_F' at Si^{29} in Si:B is not substantially less than that in n-type Si:P, indicating nearly equal admixture of s-type wave function for the hole wave function near the top of the valence band. Uncertainties in the precision of the free-electron calculation of the susceptibility make precise numerical comparison of the values of P_F' somewhat dangerous. Interpretation of the Schulman and Wyluda T_1 data[15] for p-type material at much lower concentration also indicates a very substantial wave-function amplitude at the Si^{29} site for the holes.

Table V also shows that the electron wave-function probability density is strongly peaked at the P^{31} nucleus in Si:P. The ratio of the average wave-function densities at the P^{31} site to the Si^{29} site is about 26:1. In the metallic range of Si:P, we have a metal consisting of a random superlattice of P^{31} metal atoms along with a distribution of Si^{29} atoms at an average distance of several angstroms from the P^{31} nucleus. The large peaking of the wave-function density at the P^{31} nucleus as compared with the Si^{29} nucleus is expected for metallic wave functions.[34]

[31] D. P. Miller, J. E. Moore, and C. R. Moore, J. Appl. Phys. 33, 2648 (1962).

[32] G. Feher, J. C. Hensel, and E. A. Gere, Phys. Rev. Letters 5, 309 (1960).

[33] A. Abragam, *The Principles of Nuclear Magnetism* (Oxford University Press, New York, 1961), Chap. 9, p. 390.

[34] N. F. Mott and H. J. Jones, *The Theory and Properties of Metals and Alloys* (Dover Publications, Inc., New York, 1958), Chap. 2, p. 79.

The wave function probability densities normalized in an atomic volume may be calculated from the wave-function densities in Table V. The appropriate atomic volume for P^{31} is the inverse of the average P^{31} impurity density in sample P-1. The resulting wave function probability density at the nucleus, normalized in an atomic volume, is 0.36×10^{-24} cm^{-3}. A comparison of this calculated P^{31} metallic state wave-function density may be made with the wave-function density at the P^{31} donor nucleus in silicon. Kohn and Luttinger[35] have calculated the wave-function density normalized in an atomic volume for the P^{31} donor atom in silicon from the experimental ESR value of the hyperfine splitting.[36] They find this wave function density to be 0.44×10^{-24} cm^{-3}. The ratio of metallic to donor value is consistent with ratios observed for other monovalent metals,[37] comparing the probability density at the nucleus in the metal with the probability density at the nucleus in the free atom.

VI. SUMMARY

Analysis of our NMR measurements in Si:P shows that the dominant interaction between nuclear spins and mobile electrons occurs via the Fermi contact part of the hyperfine interaction for concentrations of phosphorus impurities greater than 3×10^{19} cm^{-3}. The electrons can be described by a highly degenerate distribution and by a density of states appropriate to a parabolic band. They also exhibit no effects of correlation. Measured Si^{29} T_1's and Knight shifts in the metallic range obey the Korringa relation. This agreement indicates that the noncontact part of the hyperfine interaction does not change the observed relaxation rate by an amount larger than the measurement error. Thus, there is some substantial fraction of s character in the electron wave function, at least enough to insure that the contact part of the hyperfine interaction dominates. The electron wave function is strongly peaked at the P^{31} nucleus, with a probability density about 75% that appropriate to the free P^{31} "atom" in silicon.

A similar analysis of behavior of the Si^{29} system of Si:B shows that the Fermi contact interaction is dominant for boron concentrations greater than 1×10^{19} cm^{-3}. The holes also appear to be appropriately described as free, independent, and highly degenerate. The B^{11} T_1's and Knight shifts are properly related by the Korringa relation. The hole wave function appears to have somewhat less s character than the electron wave function in the metallic range, but not substantially less.

Agreement of the Si:P NMR data with the distribution model implies a random distribution of the P^{31} impurities up to 1.5×10^{20} cm^{-3}. In Si:B at boron concentrations greater than 1×10^{19} cm^{-3}, boron impurities are believed to form in clusters. The average local density in the clusters appears to be independent of concentration in the measured 2×10^{19} to 8.5×10^{19} cm^{-3} range and therefore to have a value greater than 8.5×10^{19} cm^{-3}.

Transition from nonmetallic to metallic properties in Si:P can be described in terms of the Poisson distribution model presented. From the appropriate Poisson distribution for a given donor concentration, one can determine the fraction of the crystal volume with average local hole densities greater than the metallic threshold local density. Success of this distribution model in explaining the P^{31} line shape and linewidth and the trnasition range in Si:P gives support to the hypothesis of Mott that there is a critical density which provides a sharp demarcation between nonmetallic and metallic properties.

ACKNOWLEDGMENTS

The authors thank Dr. S. H. Christensen for performing the ESR measurements and G. Schucker for making the arc spectra measurements. We are indebted to Dr. E. O. Kane for a useful discussion.

[35] W. Kohn and J. M. Luttinger, Phys. Rev. **97**, 883 (1955).
[36] R. C. Fletcher, W. A. Yager, G. L. Pearson, A. N. Holden, W. T. Read, and F. R. Merritt, Phys. Rev. **94**, 1392 (1954).
[37] W. D. Knight, in *Solid State Physics*, edited by F. Seitz and D. Turnbull (Academic Press Inc., New York, 1956), Vol. II, p. 124.